IEEE Open Access Journal of
Power and Energy

Received 26 July 2021; revised 9 November 2021 and 24 December 2021; accepted 27 December 2021.
Date of publication 6 January 2022; date of current version 24 January 2022.

Digital Object Identifier 10.1109/OAJPE.2022.3140658

A Comparison of Inverter Control Modes for Maintaining Voltage Stability During System Contingencies

THILINI HATHIYALDENIYE[1] (Member, IEEE),
UDAYA D. ANNAKKAGE[1] (Senior Member, IEEE),
NALIN PAHALAWATHTHA[2] (Member, IEEE),
AND CHANDANA KARAWITA[3] (Senior Member, IEEE)

[1]Department of Electrical and Computer Engineering, University of Manitoba, Winnipeg, MB R3T 2N2, Canada
[2]Hatch, North Sydney, NSW 2060, Australia
[3]Transgrid Solutions Inc., Winnipeg, MB R3T 6C2, Canada
CORRESPONDING AUTHOR: T. HATHIYALDENIYE (hathitmk@myumanitoba.ca)

ABSTRACT Inverter-based power sources are increasingly being connected to the power system due to the global drive towards renewable generation. This paper investigates the voltage stability of a power system where a load center is supplied by the grid through a transmission system along with an inverter-based generation located close to the load center. It is also assumed that there is no additional reactive power compensation at the load center and voltage control at Point of Common Coupling (PCC) is done by the inverter. This is challenging as the inverter has an added duty. If the inverter controllers are not designed properly, the inverter could reach its current limit following to contingencies rendering it unable to support the voltage at the PCC. This is due to the fact that once the current limit is reached, the inverter ceases to function as a voltage source. When the voltage at the PCC is not supported, the active power transfer capability of both the inverter and the grid will be reduced. An effective control method is required under such circumstances to handle the active and reactive components of the inverter current. Various strategies exist for controlling the active and reactive components of the inverter current while preserving the current magnitude at the rated value. The necessity of an adequate control strategy to sustain long-term voltage stability following a system contingency is emphasized in this research. This paper further discusses three candidate control strategies and the effectiveness of the reactive current prioritizing approach as a solution for operation upon system contingencies.

INDEX TERMS Contingencies, inverter-based generation, inverter control, reactive current prioritizing, voltage stability.

I. INTRODUCTION

ENSURING power system stability has become a challenging task with the increase of inverter-based renewable sources in the conventional grid [1]–[3]. This paper investigates the voltage stability of a power system where a load center is supplied through a transmission system with an Inverter-based generation (IBG) located close to the load center. It is also assumed that there is no additional reactive power support at the load center. The inverter is expected to be equipped with controllers to support the voltage at the controlled bus. There are three main regimes of voltage stability, namely, transient recovery period, Short-Term Voltage Stability (STVS) and Long-Term Voltage Stability (LTVS) as discussed in [4]–[6]. This research assumed that the inverter already consists controllers to give adequate transient voltage recovery performance, including fault-ride through. The problem addressed in this paper is managing the voltage stability under contingencies (i.e. post fault) and thus, this paper's interest is in LTVS.

Following a contingency, the IBG may need to increase the reactive power support in order to control the voltage at the load center. As a result, the inverter will reach its current

limit and begin to operate as a current source [7], losing its ability to support the voltage at the controlled bus. Therefore, enforcing proper control strategies is necessary to preserve the voltage stability of the power system upon contingencies. Contingencies lead to the increased impedance of the system as seen from the load center. A thorough understanding of the steady-state performance when the inverter reaches its current limit simultaneously with the increase of system impedance is thus required to develop an effective control strategy. This paper explores various options for controlling the active and reactive current under the circumstances described above. Based on this investigation, recommendations will be made to preserve the stability of the power system under such challenging situations.

II. RELATED PREVIOUS WORK

The power system is moving towards high penetration of renewable energy generation which, will offer plenty of environmental and sustainability benefits. They do, however, pose concerns to the power system stability. With the rising number of RE sources, the new grid codes establish additional requirements for RE. Mostly, IBGs are expected to provide the same grid support as conventional thermal and nuclear power plants. A substantial amount of research on RE integration, challenges, and solutions is published in the literature. This study focuses on one challenging issue that arise as a result of high penetration of IBG.

An analysis of power transfer capability limitation due to the maximum controllable current in the inverter is presented in [7]. Their conclusion implies that the power transfer capability depends on the active to reactive current ratios. Stability limitations of HVDC systems when the inverter operates with AC voltage (Vac) control mode or Reactive power (Q) control mode are discussed in [8]. The paper concludes that the current limit and over/under voltage limits of the inverter are the two main operation limitations in terms of active and reactive power transfer capability. If the inverter is intended to support the AC system voltage with the reactive power supply, the authors in [8] recommend limiting the active power to retain the inverter current within the limits. Authors in [9] highlighted active/reactive control combination to be the best support for most of the grid configurations.

Active and reactive power control methods are discussed in [10]–[12], particularly in IBG connected as distributed generation. Most of the research found in the literature focuses on issues related to transient voltage recovery especially, fault Ride-Through(FTR) or Low Voltage Ride-Through (LVRT) upon clearance of a fault [13]–[15]. Reactive power priority can inject more active and reactive power during the voltage recovery period compared to active priority control, resulting in improved frequency nadir [14]. According to the literature, most researchers suggest reactive power prioritization offers the best performance in terms of voltage stability throughout the transient voltage recovery period. This research, on the other hand, explores approaches for sustaining long-term voltage stability following system contingencies.

A method to achieve LTVS using active and reactive current prioritization is proposed in [16]. The authors have explored the phenomena of LTVS with large-scale solar photovoltaic (PV) generation. They have employed an active power limiting feature to render I_d to zero during the fault and active current (I_d) prioritization to maintain a constant active power supply during LTVS. However, this approach does not work when the voltage of the load center decreases due to the system contingencies as shown in section III-B.

Effective control strategies for inverter systems based on the system strength have been analyzed in [17]. According to their conclusions, the inverter is recommended to be operated as a voltage source. However, this paper presents that it is challenging to operate the inverter as a voltage source when the system is weak because the inverter reaches its current limit sooner due to the high reactive current (I_q) requirement. Thus, either active current or reactive current or both have to be curtailed to maintain the inverter current at the rated value.

The literature has highlighted crucial challenges related to weak power systems, and several studies recommend different control strategies to ensure voltage stability. However, there is a lack of a comprehensive mathematical analysis demonstrating the possibilities of the inverter reaching its current limit are increased during contingencies, as well as a thorough evaluation of possible current control strategies to ensure long-term voltage stability.

The goal of this study is to preserve long-term voltage stability following system contingencies. A mathematical analysis is presented in this paper to demonstrate, the inverter tends to reach its current limit upon a contingency. As a result, the load bus voltage will be more sensitive to the load impedance. Therefore, this paper emphasizes the necessity of a proper control strategy under such circumstances. Further, three current control strategies are discussed in this paper and presented that I_q prioritizing controls provide the best performance when the inverter operates as a current source.

III. STEADY STATE ANALYSIS

This section presents a steady-state analysis that forms the basis for the recommendations of this research.

A. IMPORTANCE OF ADDITIONAL INVERTER CONTROLS FOLLOWING A CONTINGENCY

Under normal operation, inverters operate as voltage sources and have the capability to regulate the voltage at the controlled bus. However, once the inverter reaches its current limit, it can no longer control the voltage at the controlled bus. Following mathematical derivation proves that there is a higher risk of inverter reaching its current limit during contingencies.

The system diagram used for the derivation is given in Fig. 1. This derivation treats the impedance of the transmission lines that connects the IBG to the load center (Z_2) as a constant. Z_1 is the impedance of the transmission system

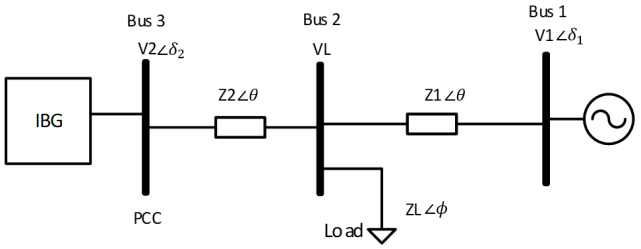

FIGURE 1. System diagram.

seen from the load bus (BUS 2). This impedance (Z_1) increases when contingencies (tripping off of lines) occur in the network.

The parameter r is the ratio of Z_2 and Z_1 as given in (1). This derivation looks for the total range of the system impedance (Z_1). In other words, it considers from the infinitely strong system (when $Z_1 = 0$ thus $r \to \infty$) to an infinitely weak system (when $Z_1 \to \infty$ and thus $r = 0$).

$$r = \frac{Z_2}{Z_1} \tag{1}$$

The voltage at the load bus (V_L) is given by

$$V_L = \frac{Z_L\angle\phi[rV_1\angle\delta_1 + V_2\angle\delta_2]}{(1+r)Z_L\angle\phi + Z_2\angle\theta} \tag{2}$$

Therefore,

$$|V_L| = \frac{Z_L\sqrt{r^2V_1^2 + V_2^2 + 2rV_1V_2\cos(\delta_2 - \delta_1)}}{\sqrt{(1+r)^2Z_L^2 + Z_2^2 + 2(1+r)Z_2Z_L\cos(\theta - \phi)}} \tag{3}$$

where; $Z_L\angle\phi$ is the magnitude and angle of load impedance, $V_1\angle\delta_1$ is the magnitude and angle of the voltage of remote grid bus (Bus 1), $V_2\angle\delta_2$ is the magnitude and angle of voltage of the inverter bus (Bus 3) and θ is the angle of the transmission line impedance.

Let S be the sensitivity of $|V_L|$ with respects to Z_L;

$$S = \frac{\partial|V_L|}{\partial Z_L} = \sqrt{\frac{A}{B}}.\frac{C}{B} \tag{4}$$

where;

$$A = [r^2V_1^2 + V_2^2 + 2rV_1V_2\cos(\delta_2 - \delta_1)] \tag{5}$$
$$B = [(1+r)^2Z_L^2 + Z_2^2 + 2(1+r)Z_2Z_L\cos(\theta - \phi)] \tag{6}$$
$$C = [Z_2^2 + 2(1+r)Z_2Z_L\cos(\theta - \phi)] \tag{7}$$

The sensitivity S is a two-variable function (of r and Z_L). The partial derivatives of S with respect to r and Z_L are given in (8) and (9).

$$\begin{aligned}\frac{\partial S}{\partial r} = {} & \frac{1}{2B^2\sqrt{AB}}.\{Z_2^4V_1[rV_1 + V_2\cos(\delta_2 - \delta_1)] \\ & + Z_2^3Z_L\cos(\theta - \phi)[r(4+3r)V_1^2 - V_2^2 \\ & + 2(2+r)V_1V_2\cos(\delta_2 - \delta_1)] \\ & + 2(1+r)^2Z_2Z_L^3\cos(\theta - \phi) \\ & \times[(1-3r)V_1V_2\cos(\delta_2 - \delta_1) \\ & - 2V_2^2 + r(1-r)V_1^2] \\ & + (1+r)Z_2^2Z_L^2\{rV_1^2[2(2+r)\cos^2(\theta - \phi) + 1 - 2r] \\ & - V_2^2[2\cos^2(\theta - \phi) + 3] \\ & + V_1V_2\cos(\delta_2 - \delta_1)[4\cos^2(\theta - \phi) + 1 - 5r]\}\end{aligned} \tag{8}$$

$$\begin{aligned}\frac{\partial S}{\partial Z_L} = {} & \frac{-(1+r)}{B^2}\sqrt{\frac{A}{B}}\{(1+r)Z_2^2Z_L[4\cos^2(\theta - \phi) + 3] \\ & + Z_2\cos(\theta - \phi)[4(1+r)Z_L^2 + Z_2^2]\}\end{aligned} \tag{9}$$

We consider only the practical range of operation. Therefore for this derivation $|V_L| \geq 0.85pu$ is used. With the condition of $|V_L| \geq 0.85pu$, it can be shown that;

$$Z_L^2 \geq 2.6Z_2^2 \tag{10}$$
$$Z_{L,min} = 1.612Z_2 = kZ_2 \tag{11}$$

where $k = 1.612$.

With the substitution of $r = 0$ and $Z_L = Z_{L,min} = kZ_2$ in (8) to consider the worst-case scenarios, it can be proven that $\partial S/\partial r$ is negative for all feasible values of r and Z_L even during the worst-case scenario. According to (9), $\partial S/\partial Z_L$ is negative regardless of the value of r or Z_L. Since both $\partial S/\partial Z_L$ and $\partial S/\partial r$ are negative, the function S does not have any local optimum points, hence the function S is monotonically decreasing function with respect to r and Z_L. Fig. 2 shows the surface plot of S and it confirms this conclusion.

System contingencies will result in decreasing r. According to this analysis, decreasing r (increasing Z_1) will result in the load bus voltage being more sensitive to load impedance (Z_L). Moreover, the analysis demonstrates that this is valid

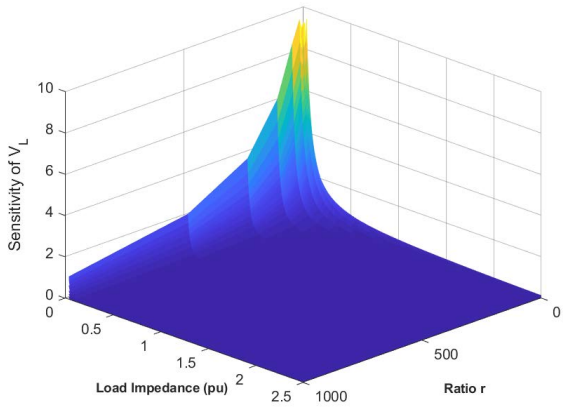

FIGURE 2. Surface plot of S (sensitivity $|V_L|$ with respects to Z_L).

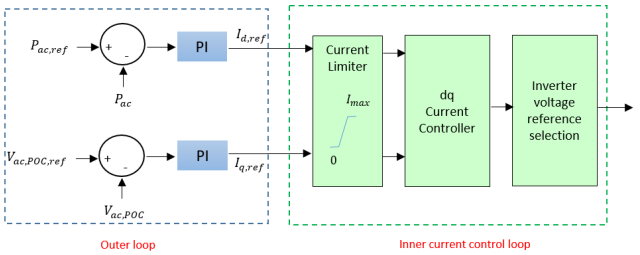

FIGURE 3. Inverter control system.

throughout the entire operating region that meets $|V_L| \geq 0.85pu$. Consequently, any network contingency will demand more reactive power from the IBG, increasing the chances of inverter reaches its current limit.

This derivation highlights the need for adequate inverter control strategies to maintain the overall system voltage stability following contingencies. Thus, the following section analyzes the steady-state behaviour of the system when the inverter approaches its current limit and reviews suitable controllers for the system to function under these conditions.

B. CURRENT CONTROL STRATEGIES

There are mainly two steps in the inverter controls; outer-loop controls and inner-loop controls as shown in Fig. 3. The outer loop controllers compare the reference values of active power and the ac side voltage magnitude with their actual values. The error goes to the corresponding PI controllers which then adjust the desired active and reactive components of the current (I_d and I_q). Then, current limiting is enforced on the current references at the inner loop controls to protect the inverter from overcurrents. If the current demanded by the outer loop is less than the rated current, the inner loop controller generates the desired magnitude and phase of the reference ac waveform for the switching controller. In this case, the inverter acts as a voltage source.

If the demanded current is greater than the rated current, the current reference is adjusted and the inner loop controllers synthesize a voltage waveform to maintain a constant current, hence, the inverter acts as a current source with a constant current magnitude. The magnitude of the inverter current (I_{inv}) is the rated current of the inverter (I_{rated}) as shown in (12). Consequently, the inverter must limit its active current, reactive current, or both to maintain the inverter current at the limit, hence the phase angle depends on the control strategy used to control the inverter current.

$$|I_{inv}| = \sqrt{I_d^2 + I_q^2} = I_{rated} \tag{12}$$

When the inverter begins to operate as a current source, it loses the ability to control the voltage at the controlled bus (PCC), causing the load bus voltage to decline rapidly. As a result, effective current control methods are necessary throughout the inverter's current source operation to regulate the voltage at the PCC and thus preserve the load bus voltage within acceptable limits. In other words, try to make the load bus voltage least sensitive to the load active power. Three candidate current control strategies are considered in this paper, and the most suitable current control method will have the lowest sensitivity of load bus voltage to load active power.

This section discusses three candidate control strategies, and the procedure of obtaining the sensitivity of load bus voltage to load active power, to ascertain the most promising current control approach. The following derivation is to obtain the sensitivity of the load bus voltage to the load active power ($\Delta V_L/\Delta P_L$). This sensitivity depends on the current control strategy. An expression for the sensitivity can be obtained by combining the linearized network equations, and the linearized equations corresponding to the current control strategy.

The network equations (13)-(19) are written considering the system described in Fig. 1 and they are common for all three current control strategies.

$$P_C = P_L - \frac{V_L}{Z_1}(V_1 cos(\delta_L + \theta) - V_L cos(\theta)) \tag{13}$$

$$Q_C = P_L tan(\phi) - \frac{V_L}{Z_1}(V_1 sin(\delta_L + \theta) - V_L sin(\theta)) \tag{14}$$

$$P_C = I_2 V_L cos(\delta_L - \alpha_2) \tag{15}$$

$$Q_C = I_2 V_L sin(\delta_L - \alpha_2) \tag{16}$$

$$V_2 cos(\delta_2) = V_L cos(\delta_L) + I_2 Z_2 cos(\alpha_2 + \theta) \tag{17}$$

$$V_2 sin(\delta_2) = V_L sin(\delta_L) + I_2 Z_2 sin(\alpha_2 + \theta) \tag{18}$$

$$\alpha = \delta_2 - \alpha_2 \tag{19}$$

P_C and Q_C are the active and reactive power at the load bus coming from the inverter side. P_L is the load active power, $V_L\angle\delta_L$ is the magnitude and angle of the load bus voltage (Bus 2), $I_2\angle\alpha_2$ is the magnitude and angle of the inverter current and α is the power factor angle of the inverter.

Equations (13)-(19) are linearized around an operating point and given in (20)-(26).

$$[2V_L^0 cos(\theta) - V_1 cos(\delta_L^0 + \theta)]\Delta V_L + Z_1 \Delta P_L + V_1 V_L^0 sin(\delta_L^0 + \theta)\Delta\delta_L - Z_1 \Delta P_C = 0 \tag{20}$$

$$[2V_L^0 sin(\theta) - V_1 sin(\delta_L^0 + \theta)]\Delta V_L + Z_1 tan(\phi)\Delta P_L - V_1 V_L^0 cos(\delta_L^0 + \theta)\Delta\delta_L - Z_1 \Delta Q_C = 0 \tag{21}$$

$$I_2 cos(\alpha_2^0 - \delta_L^0)\Delta V_L + I_2 V_L^0 sin(\alpha_2^0 - \delta_L^0)\Delta\delta_L - \Delta P_C - I_2 V_L^0 sin(\alpha_2^0 - \delta_L^0)\Delta\alpha_2 = 0 \tag{22}$$

$$-I_2 sin(\alpha_2^0 - \delta_L^0)\Delta V_L + I_2 V_L^0 cos(\alpha_2^0 - \delta_L^0)\Delta\delta_L - \Delta Q_C - I_2 V_L^0 cos(\alpha_2^0 - \delta_L^0)\Delta\alpha_2 = 0 \tag{23}$$

$$cos\delta_L^0 \Delta V_L - V_L sin\delta_L^0 \Delta\delta_L - I_2 Z_2 sin(\alpha_2^0 + \theta)\Delta\alpha_2 + V_2^0 sin\delta_2^0 \Delta\delta_2 - cos\delta_2^0 \Delta V_2 = 0 \tag{24}$$

$$sin\delta_L^0 \Delta V_L + V_L cos\delta_L^0 \Delta\delta_L + I_2 Z_2 cos(\alpha_2^0 + \theta)\Delta\alpha_2 - V_2^0 cos\delta_2^0 \Delta\delta_2 - sin\delta_2^0 \Delta V_2 = 0 \tag{25}$$

$$\Delta\delta_2 - \Delta\alpha_2 - \Delta\alpha = 0 \tag{26}$$

The equations (20)-(26) are common for all the three candidate control strategies. Since these 7 equations have

9 variables, one more equation is essential to determine $(\Delta V_L/\Delta P_L)$. The 8th equation can be obtained by considering the current control strategy as discussed in the following section.

1) ID (ACTIVE POWER (P)) PRIORITIZING CONTROL

The outer loop control determines the amount of I_d required to deliver the desired active power and the amount of I_q required to hold the controlled bus voltage magnitude (or reactive power) at the specified threshold. However, the I_d prioritization controller allows the system to supply the necessary I_d while decreasing I_q to maintain the constant current magnitude at the inner loop as illustrated Fig. 4. The inverter power factor angle α for I_d prioritizing control, can be expressed as in (27).

$$cos\alpha = \frac{P_{rated}}{S_{rated}} \tag{27}$$

The linearized equation of (27), is given in (28)

$$\Delta\alpha = 0 \tag{28}$$

By combining the equations (20)-(26) and (28), the magnitude of the sensitivity of load bus voltage to load active power for the I_d prioritizing control is given in (29).

$$\left|\frac{\Delta V_L}{\Delta P_L}\right|_P = \frac{K_1}{K_2} \tag{29}$$

where;

$$\begin{aligned} K_1 = {} & \frac{-sec(\phi)}{I_2 V_L^0 V_1 V_2^0 sin(\alpha_2^0+\theta)}\{I_2 Z_1 cos(\alpha_2^0+\phi-\delta_L^0) \\ & \times[V_L^0 cos(\delta_2^0-\delta_L^0)-V_2^0]-V_1 V_2^0 cos(\delta_2^0+\theta-\phi)\} \end{aligned} \tag{30}$$

$$\begin{aligned} K_2 = {} & \frac{-1}{I_2 V_L^0 V_1 V_2^0 Z_1 sin(\alpha_2^0+\theta)}.\{2I_2 V_1 V_2^0 Z_1 cos(\alpha_2^0+\theta) \\ & +I_2 Z_1[2V_L^0 cos(\alpha_2^0+\phi-\delta_L^0)-I_2 Z_1] \\ & \times[V_L^0 cos(\delta_2^0-\delta_L^0)-V_2^0] \\ & +V_1^2 V_2^0-2V_1 V_2^0 V_L^0 cos\delta_L^0 \\ & -I_2 V_1 V_L^0 Z_1 cos(\alpha_2^0+\theta-\delta_L^0+\delta_2^0)\} \end{aligned} \tag{31}$$

2) MAINTAIN THE ID/IQ RATIO REQUESTED BY THE OUTER LOOP

This controller limits both I_d and I_q, while ensuring the I_d/I_q ratio is the same as demanded by the outer loop as illustrated Fig. 4. The inverter power factor angle α for this control strategy, can be expressed as in (32).

$$tan\alpha = \frac{Q_2}{P_{rated}} = \frac{V_2 I_2 sin\alpha}{P_{rated}} \tag{32}$$

The linearized equation of (32), is given in (33)

$$P_{rated} sec\alpha^0 tan\alpha^0 \partial\alpha = I_2 \Delta V_2 \tag{33}$$

By combining (20)-(26) and (33), the magnitude of the sensitivity of load bus voltage to load active power for the controller which maintains the same Id/Iq ratio requested by the outer loop is given in (34).

$$\left|\frac{\Delta V_L}{\Delta P_L}\right|_U = \frac{(I_2 K_3 - K_1 P_{rated} sec\alpha^0 tan\alpha^0)}{(I_2 K_4 - K_2 P_{rated} sec\alpha^0 tan\alpha^0)} \tag{34}$$

where;

$$\begin{aligned} K_3 = {} & \frac{-sec(\phi)}{V_L^0 V_1 sin(\alpha_2^0+\theta)}\{Z_1 cos(\alpha_2^0+\phi-\delta_L^0)[V_L^0 sin(\delta_2^0-\delta_L^0) \\ & +I_2 Z_2 sin(\delta_2^0-\alpha_2^0-\theta)]+V_1 Z_2 sin(\delta_2^0-\alpha_2^0-\theta) \\ & \times cos(\theta-\phi+\delta_L^0)\} \end{aligned} \tag{35}$$

$$\begin{aligned} K_4 = {} & \frac{1}{V_L^0 V_1 Z_1 sin(\alpha_2^0+\theta)}.\{[I_2 Z_1^2-2V_L^0 Z_1 cos(\alpha_2^0+\theta-\delta_L^0)] \\ & \times[V_L^0 sin(\delta_2^0-\delta_L^0)+I_2 Z_2 sin(\delta_2^0-\alpha_2^0-\theta)] \\ & +[V_1 Z_2 sin(\delta_2^0-\alpha_2^0-\theta)][2I_2 Z_1 cos(\alpha_2^0+\theta) \\ & -2V_L^0 cos\delta_L^0+V_1] \\ & +V_1 V_L^0 Z_1 sin(\alpha_2^0+\theta-\delta_L^0+\delta_2^0)\} \end{aligned} \tag{36}$$

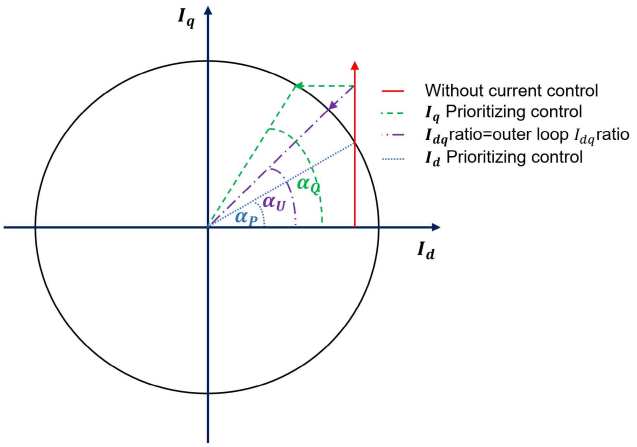

FIGURE 4. Comparison of real and reactive current behaviour for different current control modes.

3) IQ (REACTIVE POWER (Q)) PRIORITIZING CONTROL

This control provides priority to the I_q and, consequently, limits I_d to maintain a constant current magnitude as illustrated Fig. 4. The power factor angle α for I_q prioritizing control, can be expressed as in (37).

$$sin\alpha = \frac{Q_2}{S_{rated}} = \frac{V_2 I_2 sin\alpha}{S_{rated}} \tag{37}$$

The linearized equation of (37), is given in (38)

$$\partial V_2 = 0 \tag{38}$$

By combining the equations (20)-(26) and (38), the magnitude of the sensitivity of load bus voltage with respect to load active power for the I_q prioritizing control is given in (39).

$$\left|\frac{\Delta V_L}{\Delta P_L}\right|_Q = \frac{K_3}{K_4} \tag{39}$$

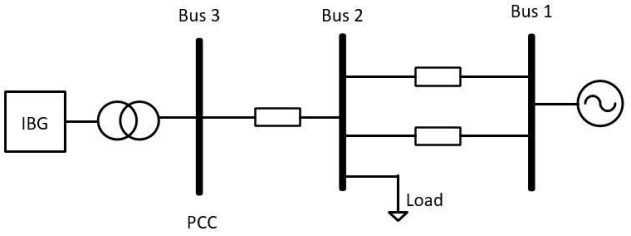

FIGURE 5. **Test system.**

The sensitivity of load bus voltage to load active power for three control strategies are given in (29),(34) and (39). However, it is not possible to determine which equation has the lowest gradient by solely examining the equations. Accordingly, the graphical illustration of the gradient is given in the result section.

IV. RESULTS

Three current control strategies were applied to the system depicted in Fig. 5, and the performances of the current controllers were evaluated.

A. SYSTEM DESCRIPTION

A remote strong grid and the nearby IBG supplying power to the load center are shown in Fig. 5. The IBG is assumed to be generating at its max capacity. The remaining amount of the load power is supplied over the two transmission lines. The grid is 100km away from the load and the IBG is located 20km away which is comparatively close to the load center. When the both transmission lines are in service (''N condition'') the SCR is 4.1 and it represents a strong transmission system. When one of the transmission lines is out of service (N-1 contingency) the SCR decreases to 2.05 and the system becomes weak. The rating of the inverter is 500MVA and is designed to operate on maximum active and reactive power at rated voltage and current. Furthermore, when the load is less than the generation of the IBG, the surplus power will be transferred to the rest of the grid over the two transmission lines.

The following conditions were used for the steady-state analysis: (a) the voltage of the grid (Bus 1) is $1\angle$ 0pu, (b) the rated active power of the inverter is 0.95pu (475MW), (c) the AC bus voltage of the inverter (Bus 3) is 1.0pu, and (d) the maximum allowable current of the inverter (I_{rated}) is 1.0pu. An inductive load with a power factor of 0.9 is used to represent the total load at the load bus. It is assumed that the voltage control at the PCC is done by the IBG during its normal operation (until the current limit is reached).

1) ID (ACTIVE POWER (P)) PRIORITIZING CONTROL

The inverter's active power vs. reactive power (PQ) curve, the inverter's voltage, current, active and reactive power variation with load active power, and the PV relationships at the load center for the N and N-1 scenarios are presented in Fig. 6, Fig. 7, and Fig. 8 respectively. Points A and B shown in Fig. 6,

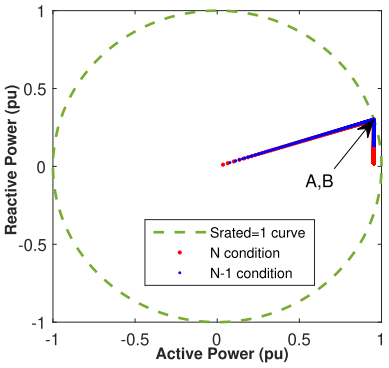

FIGURE 6. **Comparison of PQ curve of the inverter for N and N-1 conditions with I_d prioritizing control.**

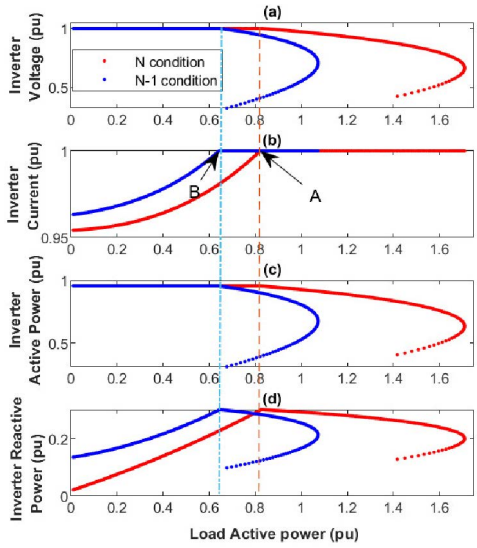

FIGURE 7. **Behaviour of the inverter (a) voltage, (b) current, (c) active power and (d) reactive power with the load for N and N-1 conditions with I_d prioritizing control. (Note: The legend in 7(a) also applies to 7(b), 7(c) and 7(d)).**

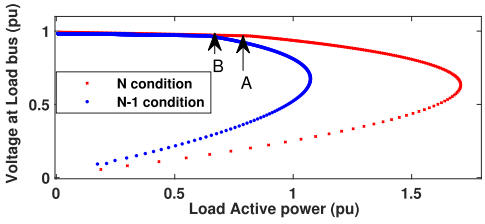

FIGURE 8. **Comparison of PV curves at load bus for N and N-1 conditions with I_d prioritizing control.**

Fig. 7, and Fig. 8 are the operating points where the inverter reaches its current limit for the two considered systems. Until then, the inverter delivers the necessary I_q (hence necessary reactive power) to hold the controlled bus voltage at the desired level and delivers the required I_d to hold the inverter active power output at the desired level as shown in Fig. 6 and Fig. 7 (a) and Fig. 7 (c).

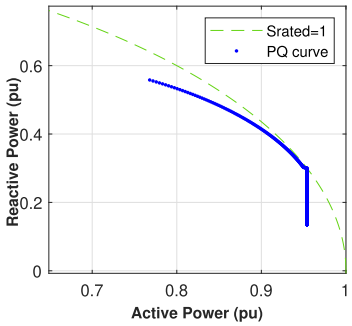

FIGURE 9. Active power vs. reactive power of the inverter when maintaining same I_d/I_q ratio requested from outer loop control.

Since the I_q is limited with I_d priority controller, the inverter cannot provide the required reactive power support to the system as illustrated in Fig. 7 (d) to maintain the voltage of the controlled bus (PCC) at the desired level and hence the voltage at the load bus. As a result, the voltage of the load bus starts to decline dramatically when the inverter approaches the current limit as shown in Fig. 8. The voltage instability issues are more prominent for the N-1 condition. This is evident in Fig. 8 as the inverter reaches the maximum current (Point B) in the N-1 contingency system before it reaches the maximum current in the original system (point A).

2) MAINTAIN THE ID/IQ RATIO REQUESTED BY THE OUTER LOOP

This controller limits both I_d and I_q while ensuring the I_d/I_q ratio is the same as demanded by the outer loop. Restricting I_q makes the inverter unable to control the voltage at the PCC, whereas limiting I_d reduces the inverter's active power supply. However, reduction of the active power supply of the inverter will allow more room for the inverter reactive power supply ($P_{inv}^2 + Q_{inv}^2 = S_{inv}^2$). Hence, the reactive power supply of the inverter will increase while the active power supply decreases as seen in Fig. 9.

The Fig. 10 (c) and (d) confirm that the inverter continues to supply reactive power requirements at the expense of active power supply once the inverter reaches its current limit at point B. The inverter bus voltage starts to drop once the inverter reaches its current limit as shown in Fig. 10 (a).

3) IQ (REACTIVE POWER (Q)) PRIORITIZING CONTROL

This controller prioritizes I_q, consequently, limits I_d to maintain a constant current magnitude. As such, the inverter's active power supply will be reduced and, a larger room is provided for the inverter's reactive power supply as seen in Fig. 11. The theoretical maximum for the I_q with this controller would be when $I_q = I_{rated}$, which leads to $I_d = 0$.

This controller provides the reactive current demand hence the necessary reactive power as illustrated in Fig. 12 (d) which needs to hold the voltage at PCC at the desired level. Most of all, the inverter with I_q prioritizing controller can control the voltage of PCC for a wider range as indicated in Fig. 12 (a).

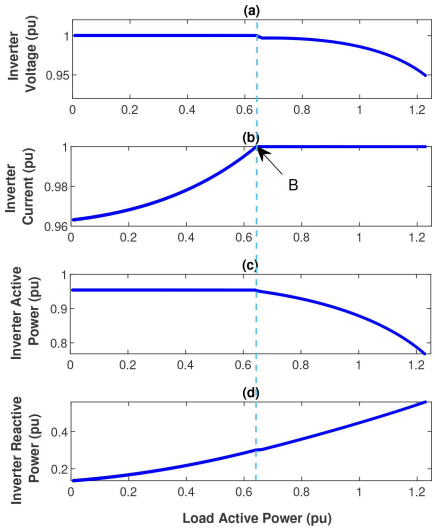

FIGURE 10. Behaviour of the inverter (a) voltage, (b) current, (c) active power and (d) reactive power with the load when maintaining same I_d/I_q ratio requested from outer loop.

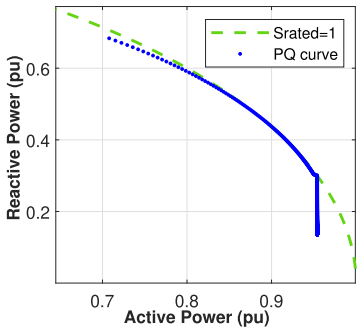

FIGURE 11. Active power vs. reactive power of the inverter when the inverter is in I_q prioritising control.

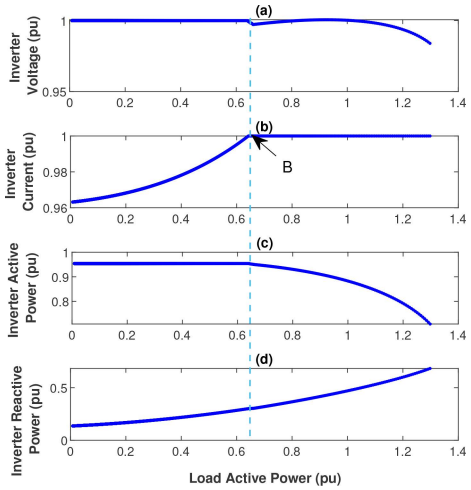

FIGURE 12. Behaviour of the inverter (a) voltage, (b) current, (c) active power and (d) reactive power with the load when the inverter is in I_q prioritising control.

The active power vs. reactive power curve of the inverter with the controller to maintain the same I_d/I_q ratio requested by the outer-loop is not on the S_{rated} circle as seen in Fig. 9.

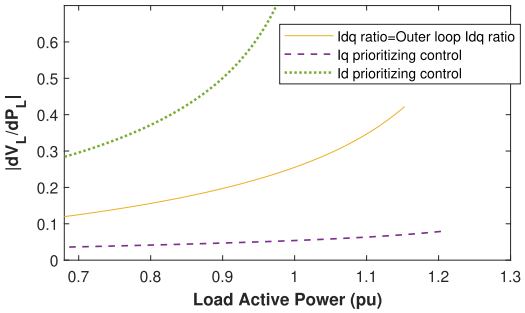

FIGURE 13. Comparison of the sensitivity of load bus voltage to load active power for different types of controllers.

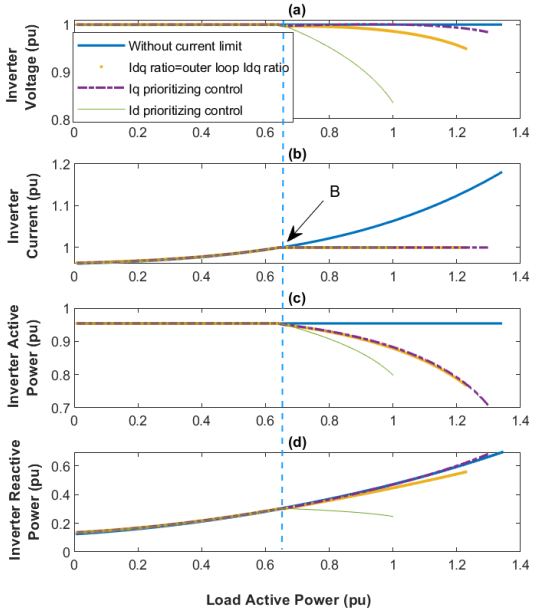

FIGURE 14. Comparison of the behaviour of inverter (a) voltage, (b) current, (c) active power and (d) reactive power for different types of controllers. (Note: The legend in 14(a) also applies to 14(b), 14(c) and 14(d)).

This indicates that the inverter performs at its rated current but not at its rated voltage ($S_{rated} = V_{rated}.I_{rated}$). Whereas, the inverter with I_q prioritizing controller operates at its rated voltage and current over a wider range of load. Hence, the active power vs. reactive power curve of the inverter is on the rated circles for a longer range of load, as shown in Fig. 11. This implies that the PCC voltage can be regulated by an inverter with I_q prioritizing control over a wider range even when the inverter functions as a current source. Therefore, the effectiveness of the I_q prioritizing controller is higher.

4) COMPARISON OF DIFFERENT INVERTER CONTROLS

The ideal inverter behaviour is attained when the inverter functions as a voltage source (with no current limit) since, it enables the inverter to sustain the voltage of PCC at the desired level while providing the desired power as illustrated in Fig. 14, Fig. 15, and Fig. 16. It was used as a reference to

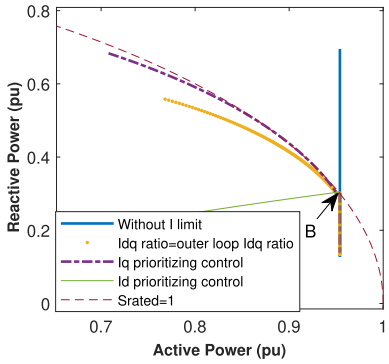

FIGURE 15. Comparison of active power vs. reactive power curves of the inverter for different types of controllers.

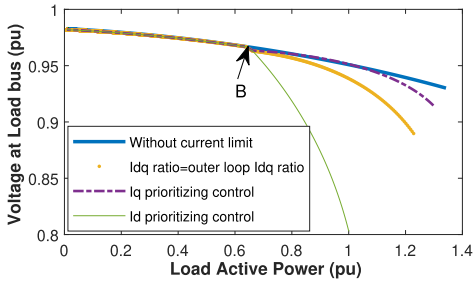

FIGURE 16. Comparison of PV curves at the load for different types of controllers.

compare with the practical situation. The closest response to the ideal behaviour is when the inverter operates with the I_q prioritization control. The Fig. 13 presents the magnitude of the sensitivity of load bus voltage to the load active power for three candidate control strategies which is plotted using (29), (34) and (39). The sensitivity of load bus voltage to load active power is lowest with I_q prioritising control, and highest with I_d prioritising control according to Fig. 13. This leads to the conclusion that, I_q priority control has higher margins for voltage stability compared to other two control methods when the inverter operates as a current source.

Table 1 provides a comparison of different current controllers for N-1 condition at the point of load bus voltage $(V_L) = 0.95pu$. With the I_q prioritization controller, the active power (P_L) and reactive power (Q_L) of the load are maintained as similar to that of an inverter operating without any current limit as given in Table 1. This is achieved by supplying the required amount of reactive power from the inverter to the system to control the voltage at the PCC, with the expense of its active power supply as seen in Fig. 14 (c) and (d) and Fig. 15. As shown in Table 1, the grid will then transmit the required amount of active power (P_{grid}) to the load when the load bus voltage is supported. The load can therefore be kept at the same level as the case where the inverter runs without a current limit. Consequently, the drop of load bus voltage is less with I_q prioritizing controller compared to the other two controllers as shown in Fig. 16.

TABLE 1. Comparison of different controllers for N-1 condition at the point of load bus voltage (V_L) = 0.95*pu*.

parameter	Without current limit	Same as outer loop I_d/I_q ratio	I_d prioritizing control	I_q prioritizing control
Z_L (pu)	0.8	0.91	1.11	0.8
P_L (pu)	1.0155	0.8927	0.7319	1.015
Q_L (pu)	0.4918	0.4344	0.3545	0.4916
P_{con} (pu)	0.95	0.9091	0.9345	0.8776
Q_{con} (pu)	0.4798	0.3986	0.311	0.4795
P_{grid} (pu)	0.0806	-0.0056	-0.1896	0.1483
Q_{grid} (pu)	0.0833	0.0901	0.1198	0.0793

Even though the I_d prioritization control attempts to retain a constant active power supply from the inverter, both the active power of the load and the load bus voltage decrease more rapidly than other two types of controllers as demonstrated in Fig. 16 and Table 1. This happens due to the inadequate reactive power support of the inverter to maintain the voltage of PCC, thus the grid must send the system a higher reactive power. However, the PCC voltage cannot be managed in the same way due to higher reactive power loss in transmission lines as the grid is far from the load center. Accordingly, the active and reactive power of the load is lowest with I_d prioritizing control. Therefore, from the voltage stability point of view, the I_d prioritization control is the worst control method and the I_q prioritization is the best.

The above study was repeated for various load power factors when the inverter operates with I_d prioritizing control and I_q prioritizing control. The results confirmed that the above behaviour is true regardless of the power factor.

V. CONTROLLER IMPLEMENTATION

The preceding part offered a steady-state study with three candidate control strategies. In this section, the test system with candidate control techniques was implemented in the Real-Time Digital Simulator (RTDS), and dynamic performance was observed.

A. TEST SYSTEM

The renewable power source in the test system described in the section III was modelled as a ±500kV, 500MW half-bridge MMC VSC HVDC system. A 10GVA high inertia synchronous generator and a 6GW load were used to represent the AC grid network. An inductive load was used to represent the total local load. The load was modelled as a step-wise increment with a step size of 25MVA. The step duration was chosen to be 1.0s to allow the system to settle to a steady-state before applying the next step load increase. The active power reference of the inverter was maintained at 475MW and the voltage reference was 1pu (230kV). DC voltage of the inverter was maintained at 500kV. The dynamic system was verified against the steady-state analysis.

B. IMPLEMENTATION

As previously explained, proper controls are required for the inverter to maintain the voltage stability of the system when the inverter reaches its current limit. The three controllers were implemented for the dynamic analysis, and the results were compared. During the normal operation, the inverter preserves the same ratio of I_d/I_q that the outer loop demands. Once the inverter reaches its current limit due to a system contingency, the control of the inverter is switched to one of these three controllers above. An additional activation controller was included to activate the required control strategy. The inverter current and the load apparent power were monitored and activation logic was created as given in Fig. 17.

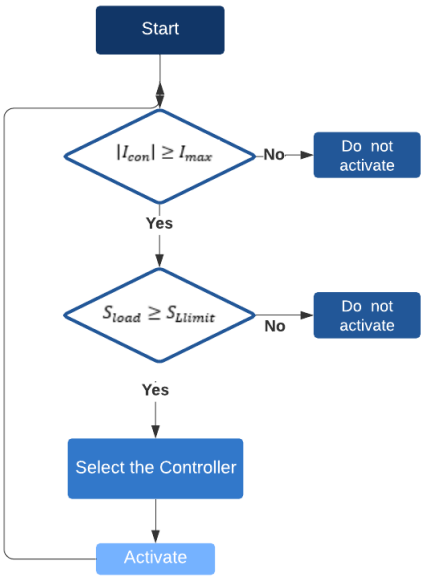

FIGURE 17. Flow chart of the supplementary inverter control.

C. RESULTS

The response of the power system to increasing load was studied with N-1 contingency. With the I_q prioritizing control, the inverter is able to supply required reactive power with less degradation of its active power supply to maintain the voltage at the load bus as seen in Fig. 18 and Fig. 19. With I_d priority control, the grid must transfer extra reactive power to the load center since the inverter cannot provide sufficient reactive power. However, the inverter readily loses the voltage control ability of the PCC with the I_d priority control, and consequently, the voltage at the load center plummets substantially, according to Fig. 20 (b) and Fig. 19. In contrast, the I_q prioritizing controller provides the required reactive power to control the voltage at the PCC, and hence has a greater capacity to maintain the voltage at the load center.

These results confirm that I_q prioritizing controller is the superior current controller out of the considered types of controllers when the inverter reaches its current limit. Therefore, this dynamic study confirms the conclusions reached with the steady-state analysis.

The effect of this I_q prioritizing controller is more significant following a contingency. Table 2 presents the maximum

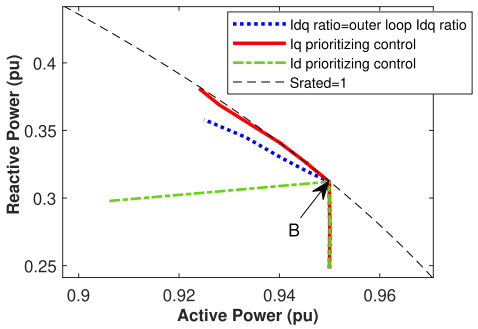

FIGURE 18. Comparison of active and reactive power curves of the inverter for different current controllers of RSACD simulation.

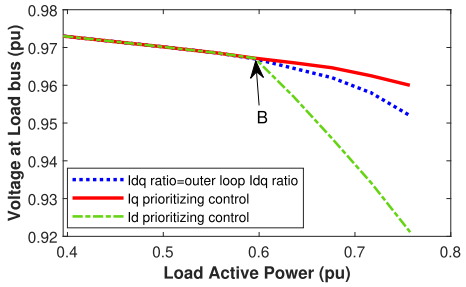

FIGURE 19. Comparison of the PV curves at load bus for different current controllers of RSACD simulation.

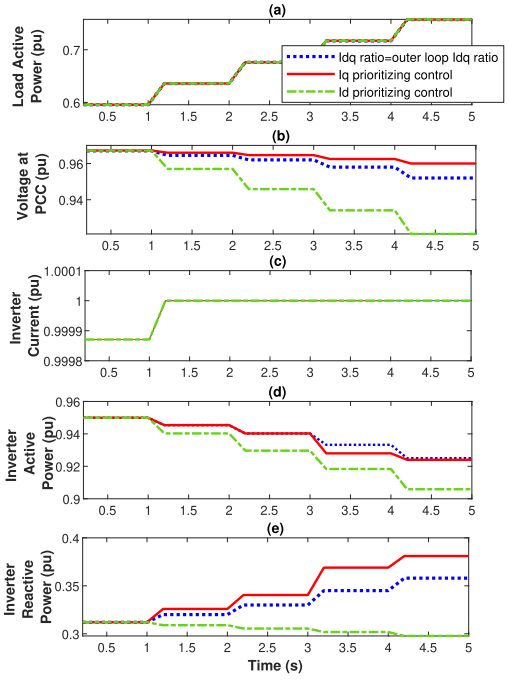

FIGURE 20. Comparison of load active power, voltage at PCC, inverter current, inverter active power, and reactive power variation for three different current controller during the N-1 contingency. (Note: The legend in 20(a) also applies to 20(b), 20(c) and 20(d)).

permissible active power supplied to the load (assuming $V_{Load} < 0.95pu$ is not acceptable) for the system with contingency for the three types of controllers. It shows the highest load power is supplied by I_q prioritizing controller

TABLE 2. Comparison of allowable maximum active power for the three types of controllers for the system with N-1 contingency.

Controllers	P_m (pu)
I_d prioritizing controller	0.701 pu
Same as outer loop I_d/I_q ratio	0.82 pu
I_q prioritizing controller	0.98 pu

compared to the other two controllers. That's because the I_q priority controller supports the load bus voltage better than the two other controllers, thus the grid can transfer the active power requirement to the load.

VI. CONCLUSION

This paper focused on ensuring long-term voltage stability, following a system contingency when the load centre is predominantly controlled by a neighbouring IBG. A mathematical analysis is provided to demonstrate that inverters tend to reach their current limit upon a system contingency, emphasizing the importance of adequate controls measures. Different control options have been analyzed to preserve long-term voltage stability following a system contingency and the I_q prioritizing controller has been selected due to its superior voltage stability performance. Dynamic simulations are presented to demonstrate the applications and conclusions obtained using the steady-state analysis. The inverter will be able to deliver more reactive power to assist the voltage at PCC by reducing its active power supply, as it acts as a current source augmented by the I_q priority controller during system contingencies. With voltage at the load bus being assisted, the grid transfers the necessary amount of active power to the load. Accordingly, the system will provide the same load, without any voltage stability concerns. Therefore the I_q prioritizing controller is an attractive option to delay investments for additional infrastructure.

REFERENCES

[1] B. Kroposki *et al.*, "Achieving a 100% renewable grid: Operating electric power systems with extremely high levels of variable renewable energy," *IEEE Power Energy Mag.*, vol. 15, no. 2, pp. 61–73, Mar. 2017.

[2] F. R. Badal, P. Das, S. K. Sarker, and S. K. Das, "A survey on control issues in renewable energy integration and microgrid," *Protection Control Modern Power Syst.*, vol. 4, no. 1, pp. 1–27, Dec. 2019.

[3] M. Liserre, T. Sauter, and J. Y. Hung, "Future energy systems: Integrating renewable energy sources into the smart power grid through industrial electronics," *IEEE Ind. Electron. Mag.*, vol. 4, no. 1, pp. 18–37, Mar. 2010.

[4] P. Kundur *et al.*, "Definition and classification of power system stability," *IEEE Trans. Power Syst.*, vol. 19, no. 3, pp. 1387–1401, Aug. 2004.

[5] N. Hatziargyriou *et al.*, "Definition and classification of power system stability revisited & extended," *IEEE Trans. Power Syst.*, vol. 36, no. 4, pp. 3271–3281, Jul. 2020.

[6] N. Hatziargyriou *et al.*, "Stability definitions and characterization of dynamic behavior in systems with high penetration of power electronic interfaced technologies," IEEE, IEEE PES Tech. Rep. PES-TR77, 2020, p. 42.

[7] L. Zeni, H. Johannsson, A. D. Hansen, P. E. Sorensen, B. Hesselbaek, and P. C. Kjaer, "Influence of current limitation on voltage stability with voltage sourced converter HVDC," in *Proc. IEEE PES ISGT Eur.*, Oct. 2013, pp. 1–5.

[8] L. Zhang, H.-P. Nee, and L. Harnefors, "Analysis of stability limitations of a VSC-HVDC link using power-synchronization control," *IEEE Trans. Power Syst.*, vol. 26, no. 3, pp. 1326–1337, Aug. 2010.
[9] S. G. Johansson, G. Asplund, E. Jansson, and R. Rudervall, "Power system stability benefits with VSC DC-transmission systems," CIGRE session B4-204, Paris, France, Tech. Rep., 2004.
[10] F. Wang, J. L. Duarte, and M. Hendrix, "Active and reactive power control schemes for distributed generation systems under voltage dips," in *Proc. IEEE Energy Convers. Congr. Expo.*, Sep. 2009, pp. 3564–3571.
[11] W. Guo, F. Liu, D. He, J. Si, R. Harley, and S. Mei, "Reactive power control of DFIG wind farm using online supplementary learning controller based on approximate dynamic programming," in *Proc. Int. Joint Conf. Neural Netw. (IJCNN)*, Jul. 2014, pp. 1453–1460.
[12] M. Ndreko, S. Rüberg, and W. Winter, "Grid forming control for stable power systems with up to 100% inverter based generation: A paradigm scenario using the IEEE 118-bus system," in *Proc. 17th Wind Integr. Workshop*, Stockholm, Sweden, 2018, pp. 17–19.
[13] M. A. Khan, A. Haque, V. S. B. Kurukuru, and M. Saad, "Advanced control strategy with voltage sag classification for single-phase grid-connected photovoltaic system," *IEEE J. Emerg. Sel. Topics Ind. Electron.*, early access, Dec. 2, 2020, doi: 10.1109/JESTIE.2020.3041704.
[14] A. Jotwani and Z. Rather, "An advanced investigation on LVRT requirement in wind integrated power systems," in *Proc. 1st Int. Conf. Large-Scale Grid Integr. Renew. Energy India*, 2017.
[15] Y. Lee and H. Song, "A reactive power compensation strategy for voltage stability challenges in the Korean power system with dynamic loads," *Sustainability*, vol. 11, no. 2, p. 326, Jan. 2019.
[16] E. Munkhchuluun, L. Meegahapola, and A. Vahidnia, "Long-term voltage stability with large-scale solar-photovoltaic (PV) generation," *Int. J. Electr. Power Energy Syst.*, vol. 117, May 2020, Art. no. 105663.
[17] S. Lu, Z. Xu, L. Xiao, W. Jiang, and X. Bie, "Evaluation and enhancement of control strategies for VSC stations under weak grid strengths," *IEEE Trans. Power Syst.*, vol. 33, no. 2, pp. 1836–1847, Mar. 2017.

THILINI HATHIYALDENIYE (Member, IEEE) received the B.Sc. (Eng.) degree from the University of Peradeniya, Peradeniya, Sri Lanka, in 2014. She is currently pursuing the Ph.D. degree with the University of Manitoba, Winnipeg, MB, Canada. She is working as a Power System Engineer with Hatch Ltd., Winnipeg.

UDAYA D. ANNAKKAGE (Senior Member, IEEE) received the B.Sc. (Eng.) degree from the University of Moratuwa, Moratuwa, Sri Lanka, in 1982, and the M.Sc. and Ph.D. degrees from the University of Manchester Institute of Science and Technology (UMIST), Manchester, U.K., in 1984 and 1987, respectively. He has more than 30 years of experience in research and teaching. He is currently a Professor with the University of Manitoba, Canada. His research expertise is in the area of power system dynamics and control.

NALIN PAHALAWATHTHA (Member, IEEE) received the B.Sc. (Eng.) degree from the University of Moratuwa, Sri Lanka, in 1981, and the Ph.D. degree from the University of Calgary, Canada, in 1988. Over 30 years, his experience covers responsibility for the operation, medium, and long-term planning of the HV electricity transmission networks, including planning of new load, generation, and distribution network connections. He also has experience in planning and specification of ancillary services as well as development of network and plant models. Over the last five years, he has been leading the connection planning and analysis on behalf of many renewable energy developers, including wind, solar, battery energy storage, hydro, and pumped hydro. He has been a member of several advisory panels and working groups for generation plant modeling, planning, and operation of high voltage networks, nationally and internationally.

CHANDANA KARAWITA (Senior Member, IEEE) is currently a professional engineer with both industrial and academic experience in power systems. He joined TGS in 2007 while doing his doctoral research at the University of Manitoba. He is well experienced in system planning studies related to HVAC, HVDC, and FACTS devices. He is also involved in state-of-the-art custom model development for HVDC and FACTS in both transient stability (PSSE, PSLF) and electromagnetic transient simulation (PSCAD) platforms. He actively contributes to various CIGRE working groups related to HVDC and FACTS, and is involved in academic research activities as an Adjunct Professor at the University of Manitoba.